The Astrophysical Journal, 627:540–549, 2005 July 1

ELECTRON HALO AND STRAHL FORMATION IN THE SOLAR WIND BY RESONANT INTERACTION WITH WHISTLER WAVES

C. Vocks,[1] C. Salem, and R. P. Lin
Space Sciences Laboratory, 7 Gauss Way, University of California, Berkeley, CA 94720

and

G. Mann
Astrophysikalisches Institut Potsdam, An der Sternwarte 16, 14482 Potsdam, Germany; cvocks@aip.de
Received 2004 October 11; accepted 2005 March 3

ABSTRACT

Observations of solar wind electron distribution functions (VDFs) reveal considerable deviations from a simple Maxwellian VDF. A thermal core and a suprathermal halo and antisunward, magnetic field–aligned beam, or "strahl," can be distinguished. At higher energies above 2 keV, a superhalo can even be observed. A kinetic description of electrons in the solar corona and wind, including resonant interaction between electrons and whistler waves, can reproduce an enhancement of suprathermal electron fluxes compared to the core flux. The whistler waves are assumed to be generated below the solar coronal base and propagate through the corona into interplanetary space. However, the resonance condition with these whistlers can only be fulfilled by electrons that move sunward. For antisunward-moving electrons, such a model lacks an efficient diffusion mechanism. The mirror force due to the opening magnetic field geometry of a solar coronal hole and in the solar wind focuses the electrons into a very narrow beam. This expectation of an extremely narrow beam is contradicted by observations of a "strahl" that has a finite width, and of an quasi-isotropic superhalo component. Thus, a diffusion mechanism for antisunward-moving electrons must exist in interplanetary space. In this paper, antisunward-propagating whistler waves are introduced into the kinetic model in order to provide this diffusion. Their wave power is estimated as a small fraction of the total wave power that is measured in interplanetary space. The kinetic results show that the whistler waves are capable of influencing the solar wind electron VDFs significantly, leading to the formation of both the halo and strahl populations and a more isotropic distribution at higher energies, in good agreement with solar wind observations.

Subject headings: diffusion — plasmas — solar wind — Sun: corona — turbulence — waves

1. INTRODUCTION

Observations of the velocity distribution functions (VDFs) of electrons in the solar wind show strong deviations from a simple drifting Maxwellian even under quiet solar conditions (see, e.g., Lin 1980). These electron VDFs display several components, a thermal core and a suprathermal halo, as well as a third antisunward magnetic field–aligned population called "strahl" (Feldman et al. 1975; Rosenbauer et al. 1977; Pilipp et al. 1987).

The 3DP (3-D Plasma and Energetic Particles Experiment) instrument on board the *Wind* spacecraft (Lin et al. 1995) observes not only the core, halo, and strahl but also a superhalo component at electron energies ranging from some keV up to 100 keV. It can be seen that the strahl vanishes at electron energies above approximately 1 keV. At higher energies above 2 keV, the superhalo appears to be isotropic (Lin 1998).

The existence of a halo population that corresponds to an enhanced number of suprathermal electrons, compared to a simple Maxwellian VDF, in the solar wind raises the question of the acceleration mechanism of the electrons. Since a coronal origin of these suprathermal tails of the electron VDF is possible (Pierrard et al. 1999), Vocks & Mann (2003) have suggested acceleration of suprathermal electrons in the solar corona by resonant interaction with whistler waves in a previous paper. The basic effect of this wave-particle interaction on the electron VDF is pitch-angle diffusion in the reference frame of the waves, resulting in the acceleration of electrons from small sunward velocities, $v_\parallel$, parallel to the background magnetic field to high speeds, $v_\perp$, perpendicular to it in the low corona where whistler wave phase speeds are high compared to the speeds of the suprathermal electrons.

The model results of Vocks & Mann (2003) show a strong enhancement of suprathermal electron fluxes in interplanetary space, which resembles the strahl component, due the whistler waves. However, this model only considers antisunward-propagating whistler waves that have been generated below the coronal base. Only electrons that move sunward ($v_\parallel < 0$) can fulfill the resonance condition with these waves. Thus, antisunward-moving electrons ($v_\parallel > 0$) do not interact with the waves.

In this model, the magnetic mirror force focuses electrons that move from the solar corona into interplanetary space up to a solar distance of 1 AU into a very narrow beam. But observations (Fitzenreiter et al. 1998) show finite strahl widths. Thus, electrons with $v_\parallel > 0$ must also experience some scattering or diffusion in interplanetary space. Since Coulomb collisions are incapable of this in the tenuous solar wind plasma, it is reasonable to assume that this diffusion is provided by plasma waves that are supplied by the interplanetary turbulence.

In this paper, an extension of the model of Vocks & Mann (2003) toward the inclusion of sunward-propagating whistler waves is presented. These whistlers are assumed to be provided by the interplanetary turbulence and lead to the diffusion of antisunward-moving solar wind electrons ($v_\parallel > 0$). We investigate whether this diffusion can limit the focusing of the electrons toward a narrow beam and yield results that coincide with the observed electron distribution functions.

[1] Now at Astrophysikalisches Institut Potsdam, An der Sternwarte 16, 14482 Potsdam, Germany.

The paper is organized as follows: In the next section, the kinetic model for electrons in the solar corona and wind, including the resonant interaction with whistler waves, is presented. Then, model results are shown and compared with *Wind* observations. The paper closes with the conclusions and summary section.

2. A KINETIC MODEL OF RESONANT INTERACTION BETWEEN ELECTRONS AND WHISTLERS IN THE SOLAR CORONA AND WIND

In a previous paper by Vocks & Mann (2003), a kinetic model for electrons in the solar corona and wind has been presented in order to investigate the acceleration of suprathermal electrons in the solar corona by resonant interaction with whistler waves. The model has been applied to the magnetic structure of a coronal funnel (Gabriel 1976) and hole that is open toward interplanetary space.

In that model, only whistler waves propagating away from the Sun have been considered. In addition to resonant interaction with electromagnetic waves, nonwavelike structures in the solar wind that support nonzero electric fields are also capable of influencing solar wind electron distributions. Such structures can be associated with interplanetary MHD turbulence (Leamon et al. 1998). However, such effects are beyond the scope of the model.

For an efficient exchange of energy between an electron and an electromagnetic wave it is necessary that the electron sees the electric field of the wave as a stationary field during its gyromotion along a background magnetic field line. This leads to the requirement that the Doppler-shifted wave frequency in the electron's reference frame equals the electron cyclotron frequency, and thus for right-hand–polarized waves to the resonance condition,

$$\omega - k_{\parallel} v_{\parallel} = \Omega_e, \tag{1}$$

where $k_{\parallel}$ is the component of the wavevector parallel to the background magnetic field and $k_{\parallel} > 0$ indicates waves propagating antisunward. The corresponding relation for left-hand–polarized waves reads $\omega - k v_{\parallel} + \Omega_e = 0$. For the electron energies covered in this paper the resonance frequencies with right-hand–polarized waves are in the whistler wave range. For left-hand–polarized, i.e., proton cyclotron waves, the resonance frequencies are very close to the proton cyclotron frequency where the waves are strongly damped by the protons. Resonance frequencies down in the MHD range are only reached for electrons with much higher energies than discussed here. Thus, whistler waves are the only wave mode propagating in the solar wind that the electrons in this model can interact resonantly with.

Since the dispersion relation of whistler waves prevents wave frequencies higher than the local electron cyclotron frequency, Ω_e, the resonance condition, equation (1), can only be fulfilled by electrons with $v_{\parallel} < 0$.

Thus, electrons with $v_{\parallel} > 0$ do not interact with the whistlers propagating away from the Sun and are focused by the mirror force into a narrow beam in interplanetary space. Such a beam formation is not supported by observations. Thus, some diffusion mechanism for electrons with $v_{\parallel} > 0$ must exist.

In this paper, the kinetic model is extended by the addition of sunward-propagating whistlers ($k_{\parallel} < 0$). According to the resonance condition, equation (1), these waves interact with electrons with $v_{\parallel} > 0$ and are capable of providing the required diffusion in interplanetary space.

2.1. *The Electron Kinetic Model*

In order to calculate electron VDFs in the solar corona and wind, a kinetic description of the electrons is necessary. The numerical method that is used in this paper has been described in detail by Vocks & Mann (2003). The basic properties of this model are repeated here for completeness.

As a kinetic model, the method is based on the solution of the Boltzmann-Vlasov equation

$$\frac{\partial f}{\partial t} + (\boldsymbol{v}\cdot\nabla) f + \left[\boldsymbol{g} - \frac{e}{m_e}(\boldsymbol{E} + \boldsymbol{v}\times\boldsymbol{B})\right]\cdot\frac{\partial f}{\partial \boldsymbol{v}} = \left(\frac{\delta f}{\delta t}\right)_{\text{Coul.}} + \left(\frac{\delta f}{\delta t}\right)_{\text{wh}}, \tag{2}$$

where $\boldsymbol{g}$ and $\boldsymbol{E}$ represent the gravitational and charge separation electric field, respectively; $\boldsymbol{B}$ is the background magnetic field, and the terms on the right-hand side are diffusion terms due to Coulomb collisions and the resonant interaction of the electrons with whistler waves.

The Coulomb collisions between the electrons and both protons and electrons are calculated using the Landau collision integral (Ljepojevic & Burgess 1990). The wave-particle interaction is evaluated within the framework of quasilinear theory, as described below.

Since the electron gyroperiods are much smaller than any other characteristic timescale, it is reasonable to assume gyrotropy of the electron VDF. This assumption reduces not only the velocity coordinates to the components parallel and perpendicular to $\boldsymbol{B}$, $(v_{\parallel}, v_{\perp})$, but also the spatial coordinates to a single coordinate, s, along $\boldsymbol{B}$. This reduction of the number of coordinates greatly lessens the numerical effort of solving the Boltzmann-Vlasov equation (2).

In order to determine the charge separation electric field, $\boldsymbol{E}$, and the parameters for Coulomb collisions with protons, a background model for the protons is needed. This is provided by a proton-electron fluid model of the solar corona and wind. Electron and proton temperatures are calculated using the energy equations of Hackenberg et al. (2000), and particle densities and flow speeds by a Parker style model (Parker 1958).

The Boltzmann-Vlasov equation (2) is solved by starting with an initial electron VDF and calculating the temporal evolution of the VDF by means of equation (2) until a final steady state has been reached. Thus, initial and also boundary conditions for the simulation box are needed. They are provided by the background fluid model.

It was the aim of Vocks & Mann (2003) to demonstrate that whistler waves in the solar corona can increase the flux of suprathermal electrons in the solar wind, so initial and boundary conditions close to Maxwellian VDFs have been defined. Since Maxwellian VDFs show strong gradients along the velocity coordinates at energies of a few keV that cause numerical problems, κ-distributions have been chosen instead:

$$f_{\kappa}(v_{\parallel}, v_{\perp}) = N_e \frac{\Gamma(\kappa+1)}{\pi^{3/2}(2\kappa-3)^{3/2} v_{\text{th}}^3 \Gamma(\kappa-1/2)} \times \left[1 + \frac{(v_{\parallel}-v_d)^2 + v_{\perp}^2}{(2\kappa-3)v_{\text{th}}^2}\right]^{-(\kappa+1)}, \tag{3}$$

where N_e is the electron number density, v_{th} the electron thermal speed, and v_d the drift speed parallel to the background

magnetic field. In the limit $\kappa \to \infty$ a κ-distribution is identical with a Maxwellian VDF; κ has been set to a high value of $\kappa = 100$ in the model calculations discussed here. This yields a distribution that is still close to a Maxwellian VDF.

For a self-consistent treatment of the solar coronal and wind plasma, the kinetic results for the electrons would have to be considered in the fluid model in order to adjust the charge separation electric field. However, the computer costs of such a method are forbiddingly high. Furthermore, the numerical mesh in velocity space is too coarse to accurately represent the thermal core of the electron VDF even at the lowest electron temperatures in the simulation box, e.g., in the transition region. Using a grid spacing that is fine enough to enable a sufficiently exact calculation of the electron density, drift velocity, temperature, and heat flux would further increase the computer costs. On the other hand, holding the background conditions fixed does not influence the kinetic results too much, since they are only coupled to the background conditions through the electric field and the Coulomb collision parameters.

2.2. *Resonant Interaction between Electrons and Whistler Waves*

The resonant interaction between electrons and whistler waves is evaluated within the framework of quasilinear theory (Kennel & Engelmann 1966). The basic effect of this interaction on the electron VDF is pitch-angle diffusion in the reference frame of the waves.

For whistler waves propagating parallel to the background magnetic field, and in the limit of sharp resonance, i.e., small damping $\gamma = |\mathrm{Im}\,(\omega)| \ll \mathrm{Re}\,(\omega)$, the quasilinear diffusion equation can be written as (Marsch 1998)

$$\left(\frac{\delta f}{\delta t}\right)_{\mathrm{wh}} = \frac{\partial}{\partial v_\parallel}\left\{\frac{1}{\tau} v_\perp \left[v_\perp \frac{\partial f}{\partial v_\parallel} + (v_{\mathrm{ph}} - v_\parallel)\frac{\partial f}{\partial v_\perp}\right]\right\} + \frac{\partial f}{\partial v_\perp}\left\{\frac{1}{\tau} v_\perp (v_{\mathrm{ph}} - v_\parallel)\left[v_\perp \frac{\partial f}{\partial v_\parallel} + (v_{\mathrm{ph}} - v_\parallel)\frac{\partial f}{\partial v_\perp}\right]\right\}, \tag{4}$$

where $v_{\mathrm{ph}} = \omega/k_\parallel$ is the wave phase speed and the factor $1/\tau$ represents a "collision frequency" due to the wave-particle interaction,

$$\frac{1}{\tau} = \frac{\pi}{4}\Omega_e^2 \left|\frac{v_{\mathrm{ph}}}{v_{\mathrm{ph}} - v_\parallel}\right| \hat{\mathcal{B}}_\omega, \tag{5}$$

where $\hat{\mathcal{B}}_\omega$ is the wave spectral energy density at the frequency ω, normalized to the magnetic field energy density, $B^2/(2\mu_0)$, and Ω_e is the electron cyclotron frequency, $\Omega_e = eB/m_e$.

For a given electron velocity $(v_\parallel, v_\perp)$ the wave frequency, and thus $1/\tau$ and v_{ph}, is determined by the resonance condition, equation (1).

The whistler waves that are propagating away from the Sun are assumed here to be generated below the lower boundary of the simulation box that is located in the transition region. Their spectral wave power is chosen to be in agreement with a high-frequency tail of the spectrum of ion-cyclotron waves in the coronal heating model of Vocks & Marsch (2002). This is based on the assumption that a mechanism that generates left-hand–polarized waves, i.e., ion-cyclotron waves, also produces right-hand–polarized waves, i.e., whistler waves.

The waves enter the simulation box at the lower boundary with this given spectrum and propagate upward. The evolution of the spectrum due to the change of the plasma background conditions with height and the absorption of the waves by the electrons are calculated.

2.3. *Sunward-propagating Whistler Waves*

A different approach is necessary for waves that propagate toward the Sun than letting a predefined spectrum of whistler waves enter the simulation box at its upper bound. Since the waves must be generated in interplanetary space, there is no reason to assume that their source is outside the simulation box that extends from the Sun up to a few AU. Furthermore, due to the decrease of the interplanetary magnetic field with distance from the Sun, the local electron cyclotron frequency takes its lowest value at the upper bound of the box. Since the dispersion relation of whistler waves precludes wave frequencies above the cyclotron frequency, a spectrum entering the box at its upper bound has no wave power at frequencies higher than the cyclotron frequency there. If the waves propagate into the box, the local cyclotron frequency increases, but without wave generation in the box there would be no wave power between the local electron cyclotron frequency and that at the upper bound.

In interplanetary space, the whistler wave phase speeds of some hundreds of kilometers per second are small compared to the speeds of suprathermal electrons of several thousand kilometers per second. Thus, the pitch-angle diffusion of the electrons in the reference frame of the waves is basically also just a pitch-angle diffusion in the rest frame of the simulation box. The kinetic energy of the electrons is hardly changed by this process. Thus, whistler wave damping or growth due to resonant interaction with electrons is small in interplanetary space.

Furthermore, the waves are assumed to be generated by turbulence in interplanetary space. This highly nonlinear process is beyond the scope of the model presented in this paper. For the above-mentioned reasons, the evolution of the whistler wave spectrum as the waves propagate sunward is not considered here. Instead, the wave spectrum is assumed to be constant in time, and it is chosen to be consistent with observational data of interplanetary space turbulence.

Wave generation by a turbulent cascade will produce waves that propagate in all directions, not only parallel to the background magnetic field, $\boldsymbol{B}$. Observations and models indicate the existence of oblique waves in the solar wind (see, e.g., Matthaeus et al. 1990 or Leamon et al. 1998). But the diffusion equation (4) applies only to waves that propagate parallel to $\boldsymbol{B}$. However, the inclusion of obliquely propagating waves would greatly complicate the diffusion equation (Marsch 2002) and preclude the numerical solution intended in this paper. On the other hand, the basic effects of quasilinear wave-electron interaction, i.e., pitch-angle diffusion, are found by a model that only includes waves propagating parallel to $\boldsymbol{B}$. Furthermore, for energetic particles Bieber et al. (1994) have found that parallel waves do most of the scattering and that highly oblique waves contribute very little to it. Thus, the exclusive consideration of whistlers propagating parallel to $\boldsymbol{B}$ is a strong but not excessively strong model assumption.

The first step in defining the spectrum of sunward-propagating whistlers is finding the overall wave spectrum in interplanetary space. As a reference, the global spectrum of solar wind electromagnetic fluctuations for frequencies from 10^{-6} up to 10^5 Hz of Salem (2000) is used. It is a compilation of data from different instruments on board the *Wind* spacecraft (Mangeney et al. 2001).

This frequency interval covers fluctuations from the MHD range up to electron cyclotron waves.

These data have been gathered at a solar distance of 1 AU. Since a useful simulation box for the kinetic model extends from the solar transition region far into interplanetary space, it is necessary to model the variation of this spectrum as a function of the distance from the Sun. Based on the assumption that the mechanism that generates the waves does not change significantly with solar distance, a nondimensional spectral function, $B^*_\omega(x)$, with $x = \omega/\Omega_e$, is introduced; $B^*_\omega(x)$ does not change within the simulation box. The spectral wave power can then be calculated as

$$B_\omega = \frac{B^2}{2\mu_0}\frac{1}{\Omega_e}B^*_\omega\left(\frac{\omega}{\Omega_e}\right). \quad (6)$$

The best fit to the solar wind measurements in Salem (2000) is achieved with

$$B^*_\omega(x) = 1.5\times10^{-9}x^{-2.6}. \quad (7)$$

The wave spectrum is found to be very steep, with a spectral coefficient of -2.6. For the average solar wind conditions in Salem (2000) with a magnetic field $B = 5.25$ nT at 1 AU, the combination of equations (6) and (7) results in

$$B_\omega = 1.1\times10^{-22}\left(\frac{\omega}{\Omega_e}\right)^{-2.6} \text{ J m}^{-3} \text{ s}. \quad (8)$$

For a frequency that is a fixed fraction of the local electron gyrofrequency, the spectral wave power as it is defined in equation (6) varies proportional to the magnetic field, as B changes with distance from the Sun, s. But such a dependency of the wave power on B leads to an unrealistic increase of the power toward the solar corona and too strong of a decrease at solar distances beyond 1 AU.

In order to reconcile the wave spectrum, equation (6), with observations and models of waves in the solar wind, another factor depending on the particle number density, N, is introduced:

$$B_\omega = \frac{B(s)^2}{2\mu_0}\frac{1}{\Omega_e(s)}\frac{N(1\text{ AU})}{N(s)}B^*_\omega\left(\frac{\omega}{\Omega_e}(s)\right). \quad (9)$$

This assumption seems to be somewhat arbitrary. However, it is not the objective of this paper to provide an accurate theory on the physics of wave generation in interplanetary space. The variation of the wave spectrum with distance from the Sun as described by equation (9) is in good agreement with both the model results and *Helios* data that are presented by Hu et al. (1999) and the *Ulysses* observations of Lin et al. (1998), so this model spectrum is appropriate for the kinetic study of electron diffusion in interplanetary space.

Equation (9) describes the total wave power B_ω as it is observed in interplanetary space. It contains contributions from many wave modes propagating in all directions. However, only whistler waves propagating toward the Sun ($k_\parallel < 0$) can fulfill the resonance condition, equation (1), with electrons that move away from the Sun ($v_\parallel > 0$).

It is reasonable to assume that at small frequencies only a minor fraction, e.g., 1%, of the total wave power at a given frequency can be assigned to sunward-propagating whistler waves. The rest can be in other wave modes, propagating parallel or perpendicular to the background magnetic field, or obliquely to $\boldsymbol{B}$.

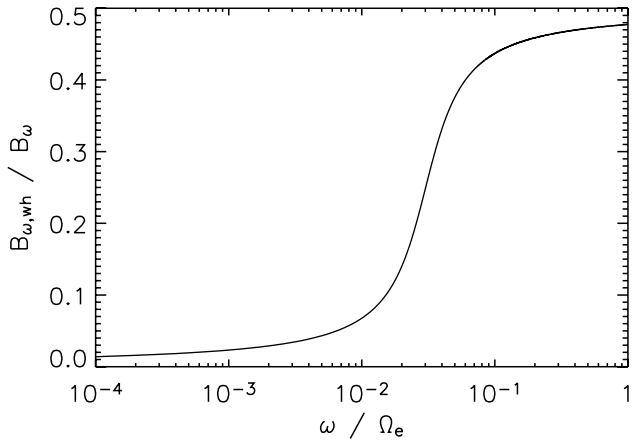

FIG. 1.—Contribution of sunward-propagating whistler waves to the total wave power in interplanetary space as a function of the wave frequency, ω, normalized to the electron cyclotron frequency, Ω_e.

This is different at frequencies above the lower hybrid frequency $\omega_{LH} = (\Omega_p\Omega_e)^{1/2}$, with Ω_p being the proton cyclotron frequency. Since the plasma frequency, ω_p, is much higher than the electron cyclotron frequency in the solar corona and wind, no wave mode can propagate perpendicular to the background magnetic field in the frequency interval $\omega_{LH} < \omega < \Omega_e$. Only electron cyclotron/whistler waves can propagate parallel to $\boldsymbol{B}$ at these frequencies. Thus, the contribution of sunward-propagating whistler waves to the total wave power can increase up to 50%. In order to avoid numerical problems with a discontinuous change of the contribution, a smooth transition is set up.

Figure 1 shows the fraction $B_{\omega,wh}/B_\omega$ of the total wave power that is assigned to sunward-propagating whistler waves as a function of frequency. At low frequencies, this fraction is of the order of 1% and increases rapidly at the lower hybrid frequency, $\omega_{LH} = 0.023\Omega_e$, toward values up to 50%.

In the kinetic calculations, the wave power of the sunward-propagating whistlers is defined as the fraction of the total wave power (eq. [9]) that is displayed in Figure 1. This whistler wave power is used to determine the "collision frequency" $1/\tau$ in equation (5) and to evaluate the electron diffusion term, equation (4).

3. KINETIC RESULTS AND COMPARISON WITH *WIND* DATA

The kinetic model for electrons that has been presented in the previous section is now applied to the plasma in the solar corona and wind. The solar coronal magnetic field configuration in the model calculations is open toward the interplanetary space, representing a coronal hole. Since coronal holes are well known as the sources of the fast solar wind, the model results are compared with observations of electron VDFs in the fast solar wind.

3.1. *The Simulation Box*

For all simulation results presented in this paper, the simulation box extends from the upper transition region at a temperature level of 7×10^5 K up to 3.9 AU in interplanetary space. Due to the assumption of a gyrotropic electron VDF, the computational domain is composed of one spatial coordinate, s, along the background magnetic field $\boldsymbol{B}$, and two velocity coordinates, $v_\parallel$ and $v_\perp$, parallel and perpendicular to $\boldsymbol{B}$, respectively. A value of $s = 0$ corresponds to the lower boundary of the simulation box in the transition region.

The magnetic field geometry in the low corona is described by the coronal funnel model of Hackenberg et al. (1999). It describes a magnetic structure that is open toward the solar wind and is characterized by a rapid expansion of the magnetic flux tube in the transition region and low corona (Gabriel 1976). Toward the solar wind, the magnetic field decreases radially as $B \propto r^{-2}$, with r being the distance from the solar center.

The spatial grid step size Δs of the computational mesh increases from 120 km in the transition region up to 0.62 AU at 3.9 AU. At a solar distance of 1 AU, $\Delta s = 0.18$ AU. The simulation results are to be compared with *Wind* data collected at 1 AU. In order to avoid any influence of the upper boundary of the box on the simulation results there, the box extends much farther out into interplanetary space.

The velocity coordinates cover electron speeds up to $0.15c$. This corresponds to an electron energy of 5.7 keV. The main objective of this paper is to study the formation of the electron strahl at much lower energies $E < 1$ keV. This choice of the velocity range of the box prevents the model results from being influenced by the high-speed boundaries of the box. The velocity grid step sizes are equidistant with $\Delta v_{\parallel} = \Delta v_{\perp} = 1500$ km s^{-1}. This is a considerable fraction of the electron thermal speed, e.g., $v_{\rm th} = 3893$ km s^{-1} for $T = 10^6$ K. But it is not the aim of this model to resolve the thermal core of the electron VDF accurately. Smaller Δv would increase the computer costs both due to the higher number of grid points and because they enforce smaller time steps Δt in iterating toward a solution of the Boltzmann-Vlasov equation (2) that is stationary in time. Since a simulation run already takes more than 1 week with $\Delta v_{\parallel} = \Delta v_{\perp} = 1500$ km s^{-1} on a Beowulf cluster, a reduction of the Δv is not feasible.

The whistler waves that propagate away from the Sun are assumed to be generated below the transition region and enter the simulation box at the lower bound (Vocks & Mann 2003). They have a power-law spectrum $\propto \omega^{-1}$, and the wave power is chosen to be in agreement with models of solar coronal heating by ion cyclotron resonance, as described in the previous section. As the waves propagate upward, the spectral evolution due to changing plasma background conditions and absorption by the electrons is considered.

3.2. *Simulation Results without Sunward-propagating Whistlers*

The first simulation run does not include sunward-propagating whistlers. It just reproduces the calculations of Vocks & Mann (2003). A comparison of the results with those of simulation runs including sunward-propagating whistlers will allow an identification of the effects of these whistlers on the electron VDF in interplanetary space.

Figure 2 shows the resulting electron VDF at $s = 0.96$ AU. The isolines are chosen in such a way that they would form equidistant circles for a Maxwellian VDF. Due to the assumption of gyrotropic electron VDFs, the velocity coordinates are cylindric coordinates, so that $v_{\perp}$ only takes positive values. But in order to increase the legibility of the plot, negative $v_{\perp}$ have been added by mirroring the VDF: $f(v_{\parallel}, -v_{\perp}) = f(v_{\parallel}, v_{\perp})$.

In the solar corona, the resonant interaction with antisunward-propagating whistler waves accelerates electrons from low speeds $v_{\parallel} < 0$ to high $v_{\perp}$. The mirror force in the opening magnetic structure of the coronal funnel and hole pushes these electrons toward positive $v_{\parallel}$, leading to an enhancement of the flux of suprathermal electrons at 1 AU. However, these electrons are focused into a narrow beam at all energies from the thermal core up to the maximum value of 5.7 keV in the simulation box. The narrowness of the beam is only limited by the resolution of the computational mesh. This results in the strong numerical oscillations that can be seen adjacent to the beam in Figure 2.

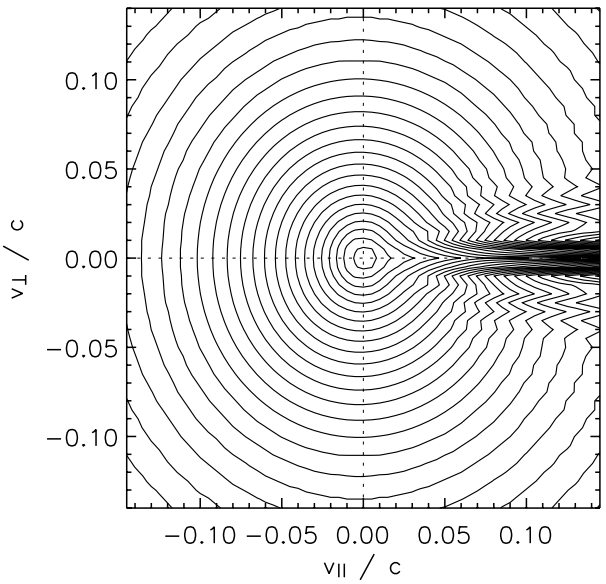

FIG. 2.—Isolines of the electron VDF at $s = 0.96$ AU from the simulation run without sunward-propagating whistler waves.

The formation of the beam is a consequence of the mirror force the electrons experience in the large-scale decrease of the solar wind magnetic field with distance from the Sun. In this simulation run there is no other effect acting on the electron VDF in the velocity range $v_{\parallel} > 0$. Due to the resonance condition, equation (1), the antisunward-propagating whistlers cannot interact with these electrons.

Figure 3 shows a cut of the electron VDF in Figure 2 along the line $v_{\perp} = 0$. A Maxwellian VDF with the same electron density and temperature is plotted for comparison. For $v_{\parallel} < 0$, it hardly differs from the Maxwellian VDF. In the range of $v_{\parallel} > 0$, the electron beam is clearly seen, but according to Figure 2 it is restricted to the case $v_{\perp} = 0$ that is chosen here. It will be interesting to compare Figure 3 with a corresponding plot of the results of a simulation run including sunward-propagating whistlers.

3.3. *Wind Observations of Electron VDFs in the Fast Solar Wind*

The extreme focusing of the electrons toward a narrow beam in a model that does not consider any electron diffusion in the velocity range $v_{\parallel} > 0$ is not confirmed by observations. Here we use observations provided by EESA-Low (EESAL), one of the electron electrostatic analyzers of the 3DP experiment (Lin et al. 1995) on board the *Wind* spacecraft. EESAL measures full three-dimensional electron VDFs with a pitch-angle resolution of 22°.

Figure 4 shows electron VDFs that have been recorded by EESAL at four different dates in the fast solar wind. The plots cover the energy range up to 1 keV. At higher energies, the VDFs become isotropic.

The four plots differ in detail due to slightly different solar wind conditions, but they share the same basic characteristics. In all four plots, the electron strahl is clearly visible. But this beam is limited to energies below approximately 1 keV, and it shows a finite width well above the instrumental angular resolution. It is much broader than would be expected for electrons that travel

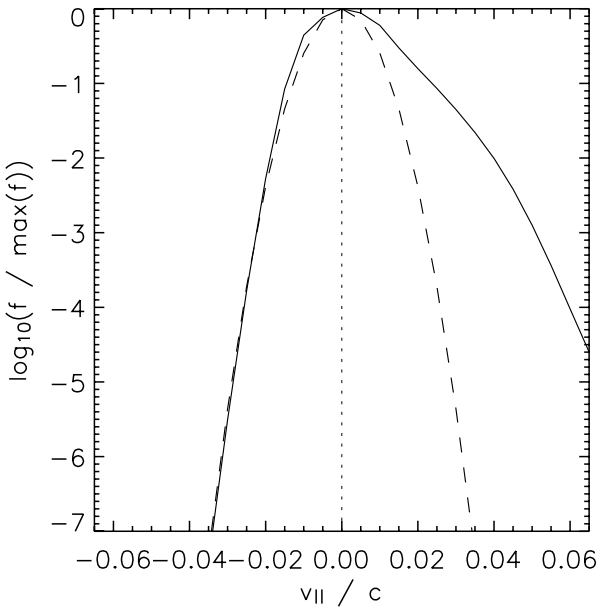

FIG. 3.—Cut along the line $v_\perp = 0$ of the electron VDF at $s = 0.96$ AU from the simulation run without sunward-propagating whistler waves (*solid line*) and Maxwellian VDF with the same density and temperature (*dashed line*).

from the solar corona toward 1 AU in interplanetary space if the beam is solely shaped by the mirror force. These observations indicate that some diffusion mechanism must act on the strahl electrons.

3.4. *Simulation Results with Sunward-propagating Whistlers*

Now the numerical solution of the Boltzmann-Vlasov equation (2) is repeated, this time under conditions of sunward-propagating whistler waves with a spectrum according to equations (7) and (9). Figure 5 shows the resulting electron VDF at $s = 0.96$ AU. The difference between the simulation runs with and without sunward-propagating whistlers is evident. Due to the action of the sunward-propagating whistlers, the electron VDF displays only small pitch-angle gradients in the range of positive $v_\parallel$, and the extremely narrow beam has disappeared. Furthermore, the spacing between the isolines of the VDF is much smaller at low speeds $v < 0.02c$ than at higher speeds. A value of $v = 0.02c$ corresponds to an electron energy of 100 eV. Since the isolines would form equidistant circles for a Maxwellian VDF, this feature can be interpreted as a thermal core and an extended halo.

Figure 6 provides a close-up view of Figure 5 for electron velocities up to $0.065c$. It enables a comparison with the *Wind* data in Figure 4.

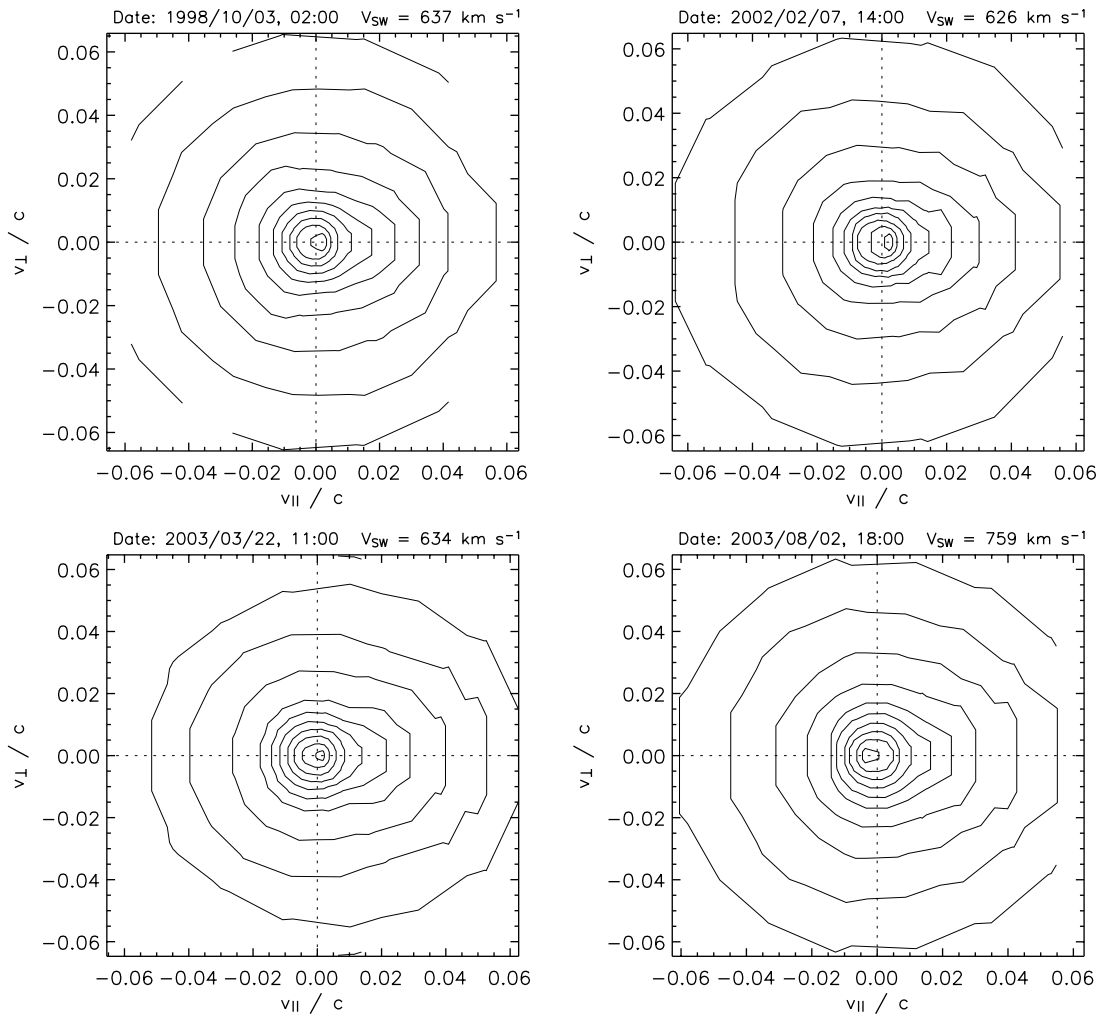

FIG. 4.—Isolines of the electron VDF as observed by *Wind* 3DP on four different dates in the fast solar wind. The dates and solar wind speeds (v_{SW}) are indicated in the plots.

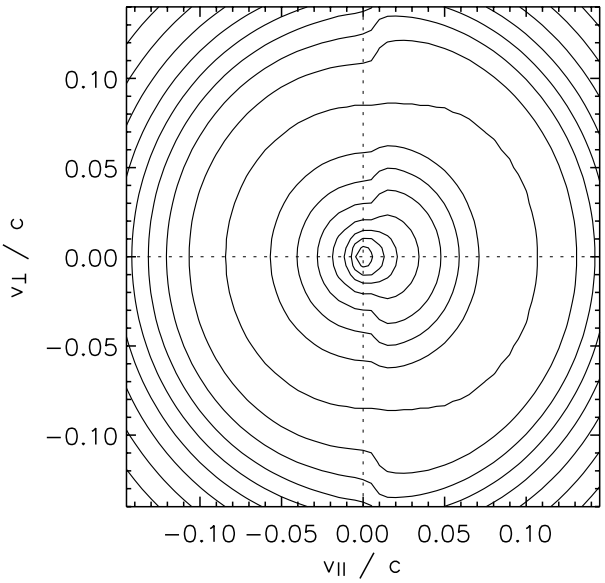

FIG. 5.—Isolines of the electron VDF at $s = 0.96$ AU from the simulation run including sunward-propagating whistler waves.

Instead of the narrow beam in the model without sunward-propagating whistlers, a strahl with a finite width has developed at low speeds $v_\parallel < 0.04c$ that is in fairly good agreement with the *Wind* observations in the fast solar wind (Fig. 4). At higher speeds, the electron distribution tends to be more isotropic.

This result shows that whistler waves can have a significant influence on the shape of solar wind electron VDFs. Despite the low spectral power of the whistlers, they can overcome the focusing by the mirror force and isotropize the distribution. The basic effect of the resonant interaction with whistlers on the electrons is pitch-angle diffusion in the reference frame of the waves, but since the whistler wave phase speeds are smaller than the electron thermal speed, this cannot be discriminated from pitch-angle diffusion in the plasma frame.

However, there is one feature in the simulation results that is not confirmed by the *Wind* observations: along the line $v_\parallel = 0$, the electron VDF in Figure 6 shows a strong pitch-angle gradient.

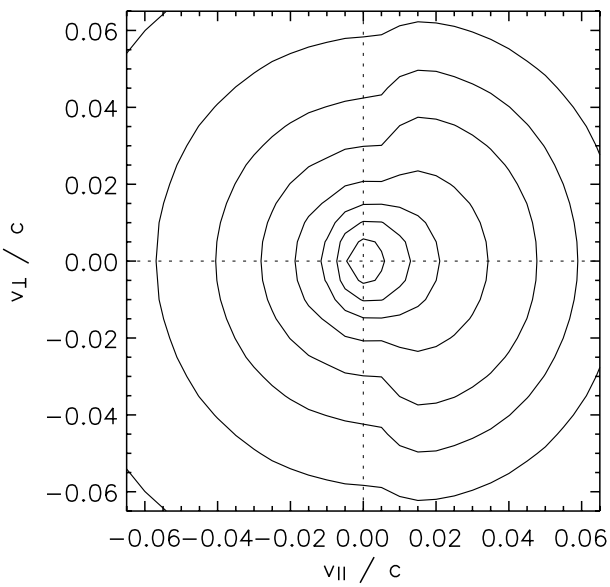

FIG. 6.—Close-up view of Fig. 5.

3.5. *Electron Diffusion across* $v_\parallel = 0$

The efficiency of the pitch-angle diffusion by resonant whistler-electron interaction depends on the "collision time" $1/\tau$ in the diffusion equation (4). The definition (5) shows that $1/\tau$ depends on the spectral wave power at the resonance frequency, $\omega_{\rm res}$. For a given electron speed $v_\parallel$, $\omega_{\rm res}$ is defined by the resonance condition, equation (1). Due to the frequency dependence of the wave phase speed, $v_{\rm ph} = \omega/k_\parallel$ and thus $k_\parallel$, this is an implicit equation for $\omega_{\rm res}$.

Only antisunward-moving electrons, $v_\parallel > 0$, can fulfill the resonance condition with sunward-propagating whistlers, $k_\parallel < 0$. The smaller the electron speed, the higher the resonance frequency. In the limit $v_\parallel \rightarrow 0$, $\omega_{\rm res}$ approaches Ω_e. The very steep wave spectrum with a spectral coefficient of -2.6 in equation (7) then has the consequence that slow electrons interact with much less wave power than faster electrons.

Figure 7 displays the collision time $1/\tau$ as a function of the electron velocity component $v_\parallel$ parallel to the background magnetic field. It can clearly be seen that $1/\tau$ sharply drops for $v_\parallel < 0.01c$. The little bulge around $v_\parallel = 0.02c$ is due to the increase of the fraction of the whistler waves in the total wave power at frequencies above the lower hybrid frequency, as shown in Figure 1.

The slow electron diffusion at $v_\parallel \rightarrow 0$ results in a low diffusion rate across the line $v_\parallel = 0$. The diffusion is more efficient at higher $v_\parallel > 0$. Since the whistler waves diffuse the electrons away from the narrow beam that forms in the simulation run without sunward-propagating whistlers, the electron phase space density at $v_\parallel > 0$ and $v_\perp > 0$ is increased compared to that simulation run. The results with and without sunward-propagating whistlers do not differ significantly at negative speeds, $v_\parallel < 0$. The lack of diffusion across the line $v_\parallel = 0$ then leads to the formation of a sharp pitch-angle gradient across $v_\parallel = 0$.

The model presented in this paper considers only the resonant interaction between electrons and whistler waves that propagate either parallel or antiparallel to the background magnetic field. As mentioned in the model description in § 2.3, the consideration of obliquely propagating waves would greatly increase the complexity of the quasilinear description and is beyond the scope of the numerical model that is employed here. It is conceivable that this simplification is responsible for the low diffusion across $v_\parallel = 0$ and thus the effective separation of the two half-spaces $v_\parallel > 0$ and $v_\parallel < 0$.

Another model assumption is the limit of sharp resonance between electrons and whistler waves, i.e., small damping $\gamma = |{\rm Im}\,(\omega)| \ll {\rm Re}\,(\omega)$ that leads to the diffusion equation (4). Bieber

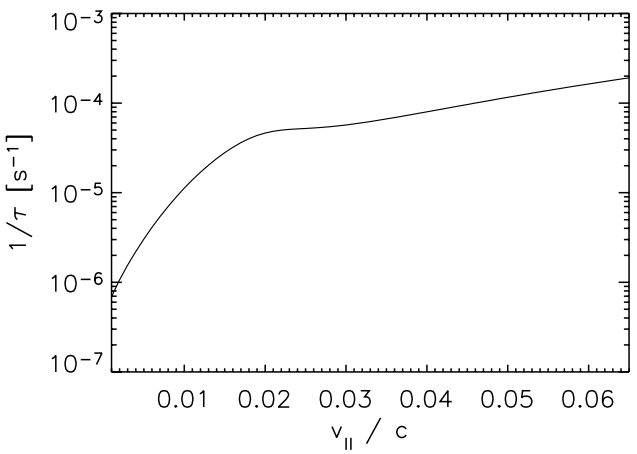

FIG. 7.—Wave-electron "collision time" $1/\tau$ as a function of $v_\parallel$ at $s = 0.96$ AU.

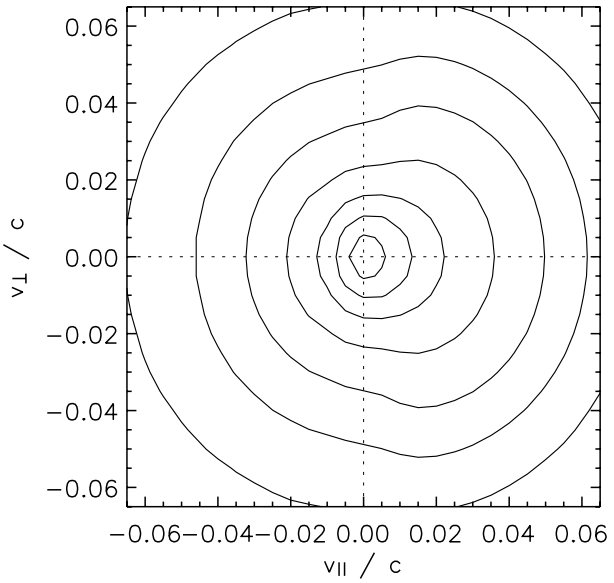

FIG. 8.—Isolines of the electron VDF at $s = 0.96$ AU from the simulation run including diffusion in $1/\tau$.

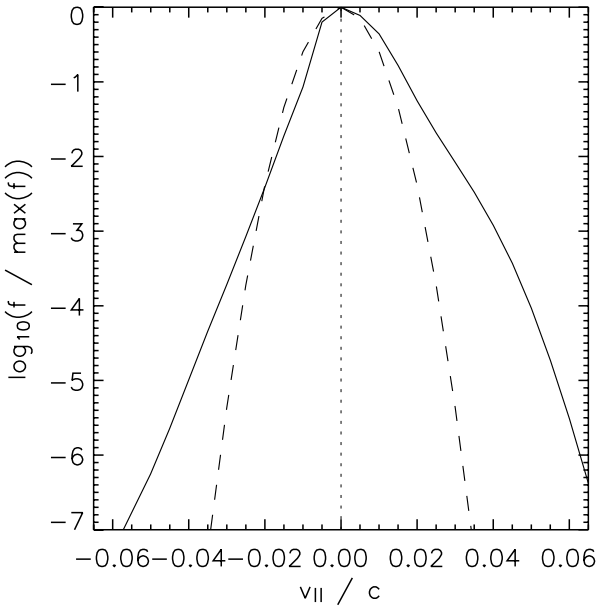

FIG. 9.—Cut along the line $v_\perp = 0$ of the electron VDF at $s = 0.96$ AU from the simulation run including diffusion in $1/\tau$ (*solid line*) and the same Maxwellian VDF as in Fig. 2 (*dashed line*).

et al. (1994) introduce dynamical effects associated with turbulence that provides a finite scattering rate at a pitch angle of 90° in order to bring the scattering theory of energetic particles in the heliosphere into agreement with observations. Dröge (2003) further investigates the role of resonance broadening and finds that it can strongly enhance the diffusion across $v_\parallel = 0$. But again the inclusion of these effects would greatly increase the complexity of the model and prevent the employment of the numerical method used here.

Thus, it is reasonable to assume that the collision time $1/\tau$ for small $v_\parallel$ is higher than is displayed in Figure 7. In order to overcome the model artifact of small $1/\tau$ for $v_\parallel \rightarrow 0$ and to represent the effects of diffusion mechanisms that are not considered here, some diffusion of $1/\tau$ along $v_\parallel$ is introduced. For each grid point i of the computational mesh $(1/\tau)_i$ is replaced by

$$\left(\frac{1}{\tau}\right)_i \rightarrow 0.4\left(\frac{1}{\tau}\right)_i + 0.2\left[\left(\frac{1}{\tau}\right)_{i+1} + \left(\frac{1}{\tau}\right)_{i-1}\right] + 0.1\left[\left(\frac{1}{\tau}\right)_{i+2} + \left(\frac{1}{\tau}\right)_{i-2}\right]. \quad (10)$$

With a grid spacing $\Delta v_\parallel = 1500$ km s^{-1} this corresponds approximately to a sliding average over the curve in Figure 7 with a window width of $0.01c$. It strongly reduces the sharp drop at small $v_\parallel$ but barely influences $1/\tau$ at higher electron speeds parallel to the background magnetic field.

Figure 8 shows the isolines of the electron VDF at $s = 0.96$ AU that has been calculated by considering the diffusion in $1/\tau$ (eq. [10]). The diffusion has greatly reduced the pitch-angle gradient across $v_\parallel = 0$.

The *Wind* observations of electron VDFs that are displayed in Figure 4 show only very small pitch-angle gradients at $v_\parallel = 0$, indicating that the efficiency of electron diffusion at $v_\parallel = 0$ is not much lower than at other pitch angles. In many cases observations show that there are even slightly more electrons on the side $v_\parallel < 0$ than on $v_\parallel > 0$, resulting in a pitch angle gradient reversed from that in Figure 8.

Pitch-angle diffusion alone tends to smooth out any pitch-angle gradient but cannot reverse it. Even if the effects of obliquely propagating whistlers were properly considered here, they could not lead to such a reversal. Thus, some other effects must play a role in these cases. One possibility is the transport of electrons parallel to the background magnetic field, $\boldsymbol{B}$, according to their $v_\parallel$. The electron speeds parallel to the background magnetic field are modified by the pitch-angle scattering, and the mirror force tends to push them toward positive $v_\parallel$. Since the electron density varies with solar distance along $\boldsymbol{B}$, it is conceivable that these dynamics influence the pitch-angle distribution of the electrons. But since the model results that are displayed in Figure 8 still show some pitch-angle gradient at small $v_\parallel$ that is not in coincidence with the *Wind* data, the investigation of such effects is beyond the scope of the current version of the electron kinetic model.

The isolines of the electron VDF in Figure 8 show a strong anisotropy between positive and negative $v_\parallel$. The isolines are extended toward higher $v_\parallel$ for $v_\parallel > 0$. This anisotropy closely resembles the strahl in the *Wind* observations (Fig. 4). The electron VDF becomes more isotropic with increasing energy, in good agreement with the *Wind* observations.

These simulation results show that the inclusion of some diffusion in $1/\tau(v_\parallel)$ alleviates the influence of the simplifying assumption of wave propagation solely parallel to the background magnetic field and leads to model results that exhibit some basic properties of solar wind electron VDFs as they are observed in interplanetary space.

Figure 9 shows a cut of the electron VDF in Figure 8 along the line $v_\perp = 0$. The figure also displays the same Maxwellian VDF as in Figure 3, obtained from the simulation run without sunward-propagating whistlers. The strahl in Figure 8 appears here as an enhancement of the electron VDF for $v_\parallel > 0$ over the corresponding $v_\parallel < 0$.

However, even for $v_\parallel < 0$ the electron VDF takes significantly higher values than the Maxwellian VDF. Its values for $v_\parallel = v$ and $v_\parallel = -v$ approach each other with increasing speed, v. This is a manifestation of the tendency of the electron VDF to become more isotropic at higher energies that was found in Figure 8.

A comparison of the electron VDF in Figure 9 with Figure 3 from the simulation run without sunward-propagating whistlers

shows that these whistlers have a strong impact on the VDF not only in the velocity range $v_\parallel > 0$ but also in the range $v_\parallel < 0$. For positive $v_\parallel$, the values of the VDF are slightly reduced, since electrons are scattered away from the extremely narrow beam that has formed in the previous simulation run without sunward-propagating whistlers (Fig. 2). But for $v_\parallel < 0$, the electron VDF now is considerably enhanced above the Maxwellian VDF, in stark contrast to the previous simulation run (Fig. 3).

From the isoline plot in Figure 8 it follows that the electron VDF has higher values not only at $(v_\parallel < 0, v_\perp = 0)$, but also for all other pitch angles. These results show that the sunward-propagating whistler waves, even if their energy corresponds to a small fraction of the total wave power in interplanetary space, limit the focusing of the strahl and furthermore lead to the formation of a halo component of the electron VDF.

4. CONCLUSIONS AND SUMMARY

Kinetic models of solar wind electrons that do not include some diffusion mechanism for electrons moving away from the Sun ($v_\parallel > 0$) result in the formation of a very narrow beam of electrons that are focused by the mirror force in the opening magnetic field geometry of a solar coronal hole and in interplanetary space.

Indeed, a beamlike feature is found in spacecraft observations of fast solar wind electron VDFs, e.g., by *Helios* or *Wind*. But in undisturbed solar wind, the pitch-angle range of this strahl is much broader than would be expected from the conservation of the magnetic moment of electrons that have traveled from the solar corona to a solar distance of 1 AU. Furthermore, the strahl vanishes at higher energies above approximately 1 keV, and the electron distribution becomes isotropic. These observational findings indicate that some diffusion mechanism for solar wind electrons must be active in interplanetary space.

In this paper, the resonant interaction between electrons and sunward-propagating whistler waves is studied within the framework of quasilinear theory. Since the interaction leads to pitch-angle diffusion of electrons with $v_\parallel > 0$, it can provide the necessary compensation of the focusing effect of the mirror force. The whistler waves are assumed to be generated by interplanetary turbulence. Only a small fraction of 1% of the total wave power that is observed in interplanetary space is assigned to sunward-propagating whistler waves at low frequencies. This contribution is increased up to 50% at frequencies above the lower hybrid frequency, $\omega_{\rm LH}$, since electron cyclotron waves are the only waves that can propagate through the solar wind plasma in the frequency range $\omega_{\rm LH} < \omega < \Omega_e$.

The results of the kinetic study of electrons in the solar corona and wind under conditions of sunward-propagating whistler waves show that the whistlers significantly influence the electron VDF at 1 AU. The electrons are effectively diffused away from the extremely narrow beam at all energies in the simulation box, despite the low whistler wave power. Since the resonance frequency of whistler waves decreases with increasing electron speed, $v_\parallel$, and the spectral wave power (eq. [9]) increases with decreasing frequency, it is even possible that at higher energies the pitch-angle diffusion described here becomes so strong that beaming electron distributions are eliminated unless the whistler wave energy is very low.

The simplifying model assumptions of whistler waves propagating only parallel to the background magnetic field and a sharp resonance with small wave damping $\gamma = |{\rm Im}\,(\omega)| \ll {\rm Re}\,(\omega)$ can lead to an artificial separation between the two velocity half-spaces $v_\parallel > 0$ and $v_\parallel < 0$ that results in a strong pitch-angle gradient across the line $v_\parallel = 0$, with a higher phase space density for $v_\parallel > 0$. This separation can be reduced by introducing some diffusion of the wave-particle "collision time" $1/\tau$ along $v_\parallel$.

This modification aims at addressing the effects of obliquely propagating whistlers and other effects such as resonance broadening that enhance diffusion across the line $v_\parallel = 0$. It reduces the separation between the velocity half-spaces, but it does not entirely rule out the pitch-angle gradient at small $v_\parallel$. Electron VDFs that have been recorded by the *Wind* spacecraft in the fast solar wind show only small pitch-angle gradients there, in many cases with slightly higher phase space densities at $v_\parallel < 0$. The current version of the kinetic model cannot address this feature due to the still important simplification of considering only whistler waves that propagate parallel to the background magnetic field.

Aside from this pitch-angle gradient at small $v_\parallel$, the kinetic results are in very good agreement with electron VDFs observed by *Wind*. At energies well below 1 keV, a strahl is visible in both the simulation and spacecraft data, and at higher energies the electron distributions become isotropic. The sunward-propagating whistler waves lead to the formation of a halo component of the electron VDF, as a result of the pitch-angle diffusion of the strahl population.

These results demonstrate that whistler waves can play a significant role in interplanetary space, even if the wave power is low. They have strong implications for the transport of suprathermal electrons in the solar wind. The pitch-angle diffusion caused by the waves has the tendency to isotropize the electron VDF and thus to compensate the focusing effect of the mirror force. Furthermore, electrons that move antisunward with $v_\parallel > 0$ can be scattered to $v_\parallel < 0$ and travel back toward the Sun and interact with antisunward-propagating whistler waves in the solar wind or even in the solar corona. The waves and the mirror force can bring them back to $v_\parallel > 0$ so that they move away from the Sun again. Some electrons can be subject to several such cycles.

In this paper, the electron halo and strahl formation in the solar wind has been studied under quiet solar conditions. The background conditions and the electron VDFs produced by the model do not change in time. But energetic electrons that are emitted in solar energetic particle events can also be affected by the resonant wave-particle interaction. A study of the implications of the whistler waves for their propagation through interplanetary space is an interesting option for future work.

This work was financially supported by the Max Planck Institute for Solar System Research in Katlenburg-Lindau through an Otto-Hahn scholarship.

REFERENCES

Bieber, J. W., Matthaeus, W. H., Smith, C. W., Wanner, W., Kallenrode, M.-B., & Wibberenz, G. 1994, ApJ, 420, 294
Dröge, W. 2003, ApJ, 589, 1027
Feldman, W. C., Asbridge, J. R., Bame, S. J., Montgomery, M. D., & Gary, S. P. 1975, J. Geophys. Res., 80, 4181
Fitzenreiter, R. J., Ogilvie, K. W., Chornay, D. J., & Keller, J. 1998, Geophys. Res. Lett., 25, 249
Gabriel, A. H. 1976, Philos. Trans. R. Soc. London A, 281, 339
Hackenberg, P., Mann, G., & Marsch, E. 1999, Space Sci. Rev., 87, 207
Hackenberg, P., Marsch, E., & Mann, G. 2000, A&A, 360, 1139

Hu, Y. Q., Habbal, S. R., & Li, X. 1999, J. Geophys. Res., 104, 24819
Kennel, C. F., & Engelmann, F. 1966, Phys. Fluids, 9, 2377
Leamon, R. J., Smith, C. W., Ness, N. F., Matthaeus, W. H., & Wong, H. K. 1998, J. Geophys. Res., 103, 4775
Lin, N., Kellogg, P. J., MacDowall, R. J., Scime, E. E., Balogh, A., Forsyth, R. J., McComas, D. J., & Phillips, J. L. 1998, J. Geophys. Res., 103, 12023
Lin, R. P. 1980, Sol. Phys., 67, 393
———. 1998, Space Sci. Rev., 86, 61
Lin, R. P., et al. 1995, Space Sci. Rev., 71, 125
Ljepojevic, N. N., & Burgess, A. 1990, Proc. R. Soc. London A, 428, 71
Mangeney, A., Salem, C., Veltri, P. L., & Cecconi, B. 2001, in Space Plasmas: Multipoint Measurements versus Theory, ed. B. Warmbein (ESA SP-492; Noorwijk: ESA), 53
Marsch, E. 1998, Nonlinear Proc. Geophys., 5, 111
———. 2002, Nonlinear Proc. Geophys., 9, 69
Matthaeus, W. H., Goldstein, M. L., & Roberts, D. A. 1990, J. Geophys. Res., 95, 20673
Parker, E. N. 1958, ApJ, 128, 664
Pierrard, V., Maksimovic, M., & Lemaire, J. 1999, J. Geophys. Res., 104, 17021
Pilipp, W. G., Miggenrieder, H., Montgomery, M. D., Mühlhäuser, K. H., Rosenbauer, H., & Schwenn, R. 1987, J. Geophys. Res., 92, 1075
Rosenbauer, H., et al. 1977, J. Geophys., 42, 561
Salem, C. 2000, Ph.D. thesis, Univ. Paris
Vocks, C., & Mann, G. 2003, ApJ, 593, 1134
Vocks, C., & Marsch, E. 2002, ApJ, 568, 1030